4668

THREE-DIMENSIONAL ANALYSIS OF AIRFLOW PATTERN AND CONTAMINANT DISPERSION IN A VENTILATED TWO-ZONE ENCLOSURE

F. Haghighat, Ph.D
Associate Member ASHRAE

J.C.Y. Wang, Ph.D
Member ASHRAE

Z. Jiang

ABSTRACT

The pattern of an isothermal airflow caused by infiltration and ventilation in a three-dimensional, two-zone enclosure is investigated by numerical simulation. The two zones are separated by a partition with a door opening. Two types of boundary condition for air supply are considered: (1) the outside air uniformly infiltrates through an end-wall into the enclosure and leaves through a ceiling-mounted exhaust opening; and (2) the ventilation air flows into the enclosure through a rectangular supply opening near the floor on one of the end-walls and leaves the enclosure through the exhaust opening. For each type of boundary condition, two different exhaust opening locations, each with three door positions, are studied. Contaminant concentration distributions for different cases are also presented to illustrate the influences of the flow pattern on the removal of the contaminant generated in one of the two zones. The results show that the location of the door not only guides the direction of the air movement but also affects the strength of the air circulation in the downstream zone, while the upstream zone is less affected by the door position.

INTRODUCTION

The major aim of ventilating (mechanical and natural) spaces for human occupancy is to provide an acceptable indoor environment for humans, i.e., to distribute heat and moisture and to remove contaminants. Therefore, understanding the air movement induced by ventilation becomes extremely important in fundamental studies of building thermal analysis, indoor air quality, and thermal comfort. The airflow pattern in single ventilated enclosures has been examined by many researchers (Berne and Villand 1987; Chen et al. 1988; Davidson and Olsson 1987; Gosman et al. 1980; Horstman 1988; Kato et al. 1986; and Lemaire 1987), while little attention has been paid to the airflow pattern in two-zone enclosures. It is obvious that besides the positions of the air supply and exhaust, the door location in the partition will be an additional factor affecting the airflow pattern in each zone. Depending on the overall arrangement, a partition may either block the ventilation airflow, causing a stagnation of polluted air, or reinforce the air movement in both zones, producing a more efficient removal of indoor pollutant. Comprehending the effects of the opening locations on the flow pattern is necessary for providing a comfortable indoor environment.

For partitioned enclosures, some research works were conducted on the airflow patterns under natural convection. Kelkar and Patankar (1985) and Chang et al. (1982) investigated the natural convective heat and mass transfer in partitioned rooms by numerical simulation. In their studies, the partitions were two-dimensional. The opening on the partition ran through the whole width of the rooms, and the flow conditions were laminar. Haghighat et al. (1989) numerically studied the natural convective heat transfer and the airflow pattern in a three-dimensional partitioned enclosure under turbulent flow. They also investigated the effects of the partition locations and door locations on the airflow patterns in two-zone enclosures. In their study, it was assumed that the air movement was caused only by the temperature difference between two end-walls and that there was no air flow across the boundary of the enclosure. The airflow patterns in ventilated enclosures are completely different from those caused by natural convection. They are affected, not simply by the location of the door, but by the overall plan of the relative positions of the door, the air supply, and exhaust. So far, airflow patterns for ventilated enclosures separated by a partition with a door opening in it have not been investigated. The purpose of the present study is to investigate the airflow pattern and the contaminant dispersion in a ventilated two-zone enclosure and to examine the effect of the door position on the air movement. The following two types of mass flow boundary condition are considered: (1) air uniformly infiltrates from the outside into the enclosure through an end-wall and leaves the enclosure through a ceiling-mounted rectangular exhaust opening; (2) ventilation air enters and leaves the enclosure through supply and exhaust openings, respectively, without any air infiltration at the boundary of the enclosure.

F. Haghighat, J.C.Y. Wang, and **Z. Jiang** are all at the Center for Building Studies, Concordia University, Montreal, Quebec, Canada.

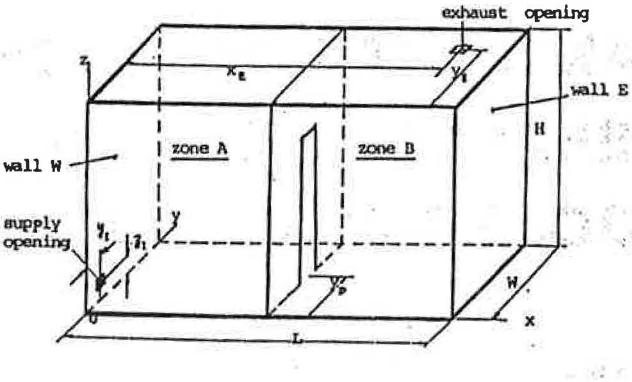

Figure 1 The configuration of a two-zone enclosure

PROBLEM STATEMENT AND GOVERNING EQUATIONS

Figure 1 presents the configuration of a typical two-zone cuboid enclosure. The dimensions of the enclosure are L × W × H = 10 × 4 × 3 m³. A partition running through the entire width of the enclosure divides the enclosure into two equal zones, zone A and zone B. The two zones are connected by a door opening in the partition. Two types of boundary condition for airflow are considered. In the first type, the outside air uniformly infiltrates into the enclosure through one of the end-walls, wall *W*, at a velocity of 0.01 m/s and leaves the enclosure through a rectangular exhaust opening placed on the ceiling. In the second type, the fresh air flows into the enclosure through a rectangular supply opening located on wall *W*, with $(y_I/W) = 0.13$ and $(z_I/H) = 0.042$, and leaves the enclosure through the exhaust opening on the ceiling. The air velocity at the supply opening is taken as 2.0 m/s (5 ach). A contaminant source with a constant emission rate (assumed unit) is placed at the height of $z_s/H = 0.125$, right under the exhaust opening for all cases.

The dimensions of the supply, exhaust, and door openings are listed in Table 1. In this study, these dimensions remain unchanged. The locations of the partition and the supply opening are also fixed for all cases, while the exhaust opening and the contaminant source are placed in zone A and zone B, respectively, as specified in the next section.

TABLE 1
Dimensions of the Opening

	Door	Supply	Exhaust
h/H	0.75	0.083	0.056 (l_E/L)
b/W	0.17	0.083	0.083

In order to simplify the problem, the following assumptions are made: (1) the thickness of the partition is small relative to the length of the enclosure and may be neglected; (2) the buoyancy force in a ventilated enclosure has a negligible effect on the flow field and may be neglected; (3) the contaminant source is considered to be a point source, namely, it does not have any physical volume; and (4) a one-phase flow is assumed in this study, that is, both the air and the contaminant (gas or particle) have the same velocity.

TABLE 2
Source Terms for Conservation Equations

ϕ	Γ_ϕ	S_ϕ
1	0	0
u	μ_{eff}	$-\partial p/\partial x + \partial/\partial x(\mu_{eff}\, \partial u/\partial x) + \partial/\partial y\, (\mu_{eff}\, \partial v/\partial x) + \partial/\partial z\, (\mu_{eff}\, \partial w/\partial$
v	μ_{eff}	$-\partial p/\partial y + \partial/\partial x(\mu_{eff}\, \partial u/\partial y) + \partial/\partial y\, (\mu_{eff}\, \partial v/\partial y) + \partial/\partial z\, (\mu_{eff}\, \partial w/\partial$
w	μ_{eff}	$-\partial p/\partial z + \partial/\partial x(\mu_{eff}\, \partial u/\partial z) + \partial/\partial y\, (\mu_{eff}\, \partial v/\partial z) + \partial/\partial z\, (\mu_{eff}\, \partial w/\partial$
k	$\frac{\mu_{eff}}{\sigma_k}$	$G_k - \rho\epsilon$
ϵ	$\frac{\mu_{eff}}{\sigma_\epsilon}$	$C_1\, \epsilon/k - C_2\, \epsilon/k$
c	$\frac{\mu_{eff}}{\sigma_c}$	0

$G_k = \mu_{eff}\, [2\, ((\partial u/\partial x)^2 + (\partial v/\partial y)^2 + (\partial w/\partial z)^2) + (\partial u/\partial y + \partial v/\partial x)^2 + (\partial u/\partial z + \partial w/\partial x)^2 + (\partial v/\partial z + \partial w/\partial y)^2]$

Generally speaking, the airflow in a ventilated enclosure is turbulent. In this study, the Reynolds number, Re is more than 3.6 × 10⁴ with u_{in} = 2.0 m/s. Therefore, the flow is turbulent (Gosman et al. 1980). Consequently the *k*-ϵ two-equation model of turbulence (Rodi 1984) is adopted. The governing equations describing three-dimensional turbulent, incompressible flow can be written in the following conservation form,

$$\frac{\partial \rho\phi}{\partial t} + \frac{\partial u_i\phi}{\partial x_i} = \frac{\partial}{\partial x_i}\left(\mu_{\phi,eff}\frac{\partial \phi}{\partial x_i}\right) + S_\phi \qquad (1)$$

where ϕ denotes the variables *u, v, w, c, k, and* ϵ, respectively. S_ϕ represents the source term for the corresponding ϕ variable and is listed in Table 2.

The boundary conditions are as follows:
for wall *W* with infiltration,

$$u = u_{IF} \qquad (2)$$

$$v = w = 0 \qquad (3)$$

$$k = 0 \qquad (4)$$

$$\partial\epsilon/\partial x = \text{constant} \qquad (5)$$

and

$$c = 0 \qquad (6)$$

for the other solid surfaces,

$$u = v = w = 0 \qquad (7)$$

$$k = 0 \qquad (8)$$

$$\partial\epsilon/\partial n = \text{constant} \qquad (9)$$

and

$$c = 0 \qquad (10)$$

for the supply opening (the second type only),

$$u = u_I \qquad (11)$$

$$v = w = 0 \qquad (12)$$

$$k = k_I = 3/2\, u_t^2 \quad \text{(where } u_t = 0.05\, u_I\text{)} \qquad (13)$$

$$\epsilon = \epsilon_I = C_\mu\, k_I^{1.5}/l \qquad (14)$$

and

$$c = 0 \qquad (15)$$

and for the exhaust opening,

$w = w_E = u_{IF} H\, W/A_E$ for the first type of air supply

$w = w_E = u_I A_I/A_E$ for the second type of air supply

$$u = v = 0 \tag{17}$$

$$c = c_E = e/(\rho u A_E) \tag{18}$$

$$\partial k/\partial z = 0 \tag{19}$$

and

$$\partial \varepsilon/\partial z = \text{constant} \tag{20}$$

NUMERICAL PROCEDURE

The numerical computation is performed on 20 × 14 × 14 uniform control volumes. The differential equations are obtained by integrating the governing equations over each of the control volumes. The Hybrid Scheme and a staggered mesh system are used for casting differential equations. The iteration procedure is carried out by the ADI method with the false time-step. As a boundary condition, the correction of a global continuity conservation is employed for the velocity component in *x* direction at the door opening. The air velocities at the supply and exhaust openings are considered to be uniformly distributed over the entire area of the openings. The turbulent wall functions (Launder and Spalding 1974) are applied to describe the properties at the grids near the solid surfaces, except for wall *W* through which the outside air infiltrates in the enclosure, because, with the air penetration, the boundary layer near this wall does not exist.

This paper will not go into the details of derivation of differential equations, since the numerical procedure adopted in this paper is similar to the one in Haghighat et al. (1989).

RESULTS

Two types of air entering conditions, as described above, are considered. For each type, six cases with different exhaust and door opening locations are examined. Twelve cases are listed in Table 3.

It should be noted that, in the classification of the cases, the first number denotes the type of air entering condition, the following capital letter indicates the zone where the exhaust opening is placed, and the last number represents the location of the three different door positions.

TABLE 3
Arrangement of the Air Inlet, Outlet, and Door Openings

First type: air infiltration through wall *W*	**Door location** y_D/W	**Exhaust location** x_E/L	y_E/W
Case 1B-1	0.17		
Case 1B-2	0.50	0.75 (zone B)	0.71
Case 1B-3	0.75		
Case 1A-1	0.17		
Case 1A-2	0.50	0.19 (zone A)	0.71
Case 1A-3	0.75		
Second type: supply opening on wall *W* at $z_I/H=0.042$, $y_I/W=0.13$	**Door Location** y_D/W	**Exhaust Opening** x_E/L	y_E/W
Case 2B-1	0.17		
Case 2B-2	0.50	0.75 (zone B)	0.88
Case 2B-3	0.83		
Case 2A-1	0.17		
Case 2A-2	0.50	0.19 (zone A)	0.88
Case 2A-3	0.83		

First Type of Entering Air

For the first type, the outside air enters the enclosure through entire wall *W* in zone A by uniform infiltration.

Exhaust and Contaminant Source in Zone B ($x_E/L = 0.75$, $y_E/W = 0.71$): Figure 2 indicates that in zone A, the airflow is nearly one-dimensional and uniform, regardless of the location of the door opening.

In zone B, however, the airflow pattern is obviously dependent on the position of the door. In case 1B-1 (Figure 2a), the air in zone B forms a large anti-clockwise vortex, centering about the exhaust opening. This vortex occupies the major area of zone B. A small clockwise circulation in the southeast corner is also seen. In case 1B-2 (Figure 2b), there exist two large circulations in zone B, one clockwise at the southeast corner and the other anti-clockwise near the northern wall. In case 1B-3 (Figure 2c), the door opening, at $y_D/w = 0.75$, is closer to the exhaust opening (see Table 3). The air, after passing through the door opening, seems to have a short way to leave the enclosure through the exhaust opening; consequently, the air movement in zone B would become weaker. However, in comparing Figure 2c with Figure 2a, there is no significant decrement of the air movement in zone B. The air still travels the entire region of zone B before leaving. The vortex, which is centered at the exhaust opening 8 in cases 1B-1 and 1B-2, does not exist in case 1B-3 (Figure 2c). Instead, there is a large, clockwise circulation in the region near wall E in zone B.

Figures 2d and 2e present the contours of the contaminant concentration in the horizontal plane at $z/H = 0.63$ for cases 1B-1 and 1B-3, respectively. The contours of contaminant concentration also follow the path of air movement in a circulation form. In case 1B-3, the source position is at the upstream region (close to the door opening), therefore the contaminant is directly diluted by the fresh air and is removed from the exhaust. Thus, the average concentration in Figure 2e is lower than that in Figure 2d.

Exhaust and Contaminant Source in Zone A ($x_E/L = 0.19$, $y_E/W = 0.71$): Generally speaking, the outside air is not likely to constantly infiltrate into a building in a fixed direction. In order to examine the flow pattern subject to the air infiltration in the opposite direction, we simply move the exhaust opening from zone B to zone A instead of changing the direction of the air infiltration.

Figure 3a demonstrates the velocity vectors for case 1A-1 in the vertical plane at $y/W = 0.17$. Figures 3b, 3c, and 3d demonstrate the velocity vectors in the horizontal plane at $z/H = 0.38$ for cases 1A-1, 1A-2, and IA-3, respectively.

From Figures 3b, 3c, and 3d, it can be seen that in zone A, the airflow pattern and the magnitude of the velocity are not significantly changed by changing the position of the door opening. The explanation of this is that, in a steady state, the location of the exhaust opening is more responsible for controlling the air movement in zone A than that of the door opening because of the mass continuity. Figures 3a and 3b indicate that only a small portion of the infiltrating air has the chance of going to zone B through the door opening, while the rest of the air forms a vortex in the northern region in zone A.

In zone B, the velocities are relatively low, because a large portion of the air never has the chance to enter zone B before it leaves the enclosure. The air forms a weak vortex in zone B. For case 1A-1 (Figure 3b), the vortex in zone B

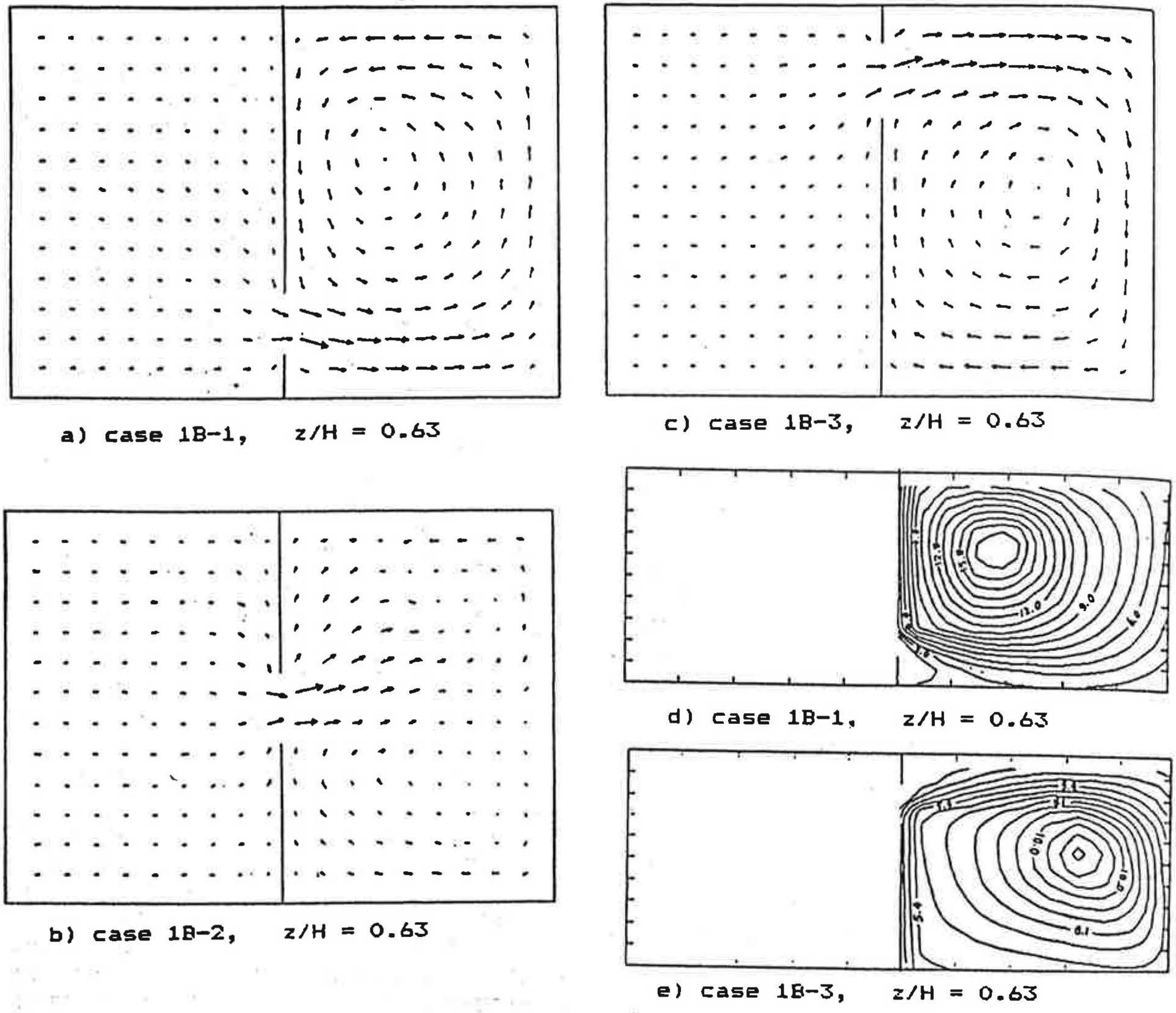

a) case 1B-1, z/H = 0.63

b) case 1B-2, z/H = 0.63

c) case 1B-3, z/H = 0.63

d) case 1B-1, z/H = 0.63

e) case 1B-3, z/H = 0.63

***Figure 2** Velocity vectors and contaminant contours for the cases with exhaust in zone B*

is anti-clockwise, while for cases 1A-2 (Figure 3c) and 1A-3 (Figure 3d), it becomes clockwise. When the door opening moves northwards along the partition, the magnitude of the air velocity in zone B decreases slightly (comparing Figure 3d with Figure 3b).

Figure 4a shows the distribution of the contaminant concentration in the horizontal plane at $z/H = 0.38$ for case 1A-3. In this case, the contaminant source ($x_S/L = 0.19$, $y_S/W = 0.71$) and door opening (centered at $y_D/W = 0.75$) are very close to each other, and the contaminant seems to have a higher probability of moving into zone B. However, the contaminant dispersion is restrained by the air vortex in zone A (see Figure 3d); therefore, the contaminant can hardly enter zone B. In Figures 4b and 4c, note that the contours at the plane of $(z/H) = 0.96$ for cases 1A-3 and 1A-1 are almost the same. This is attributed to the similarity of the flow patterns in these two cases.

Second Type of Entering Air

For the second type of entering air, the ventilation air enters the enclosure through the supply opening, whose position is fixed on wall W near the floor ($y_I/W = 0.13$, $z/H = 0.042$) for all cases. The exhaust opening and the contaminant source are placed either in zone B (cases 1B-1, 2B-2, and 2B-3) or in zone A (cases 2A-1, 1A-2, and 2A-3).

Exhaust and Contaminant Source in Zone B ($x_E/L = 0.75$, $y_E/W = 0.88$) Figure 5 illustrates the velocity vectors for cases 2B-1, 2B-2, and 2B-3. In zone A, the flow pattern does not show much difference with the variation of the door position (Figures 5a, 5c, and 5d). Only the magnitude of the velocity in this zone increases slightly from case 2B-1 (Figure 5a) to case 2B-3 (Figure 5d). In each of these horizontal planes, an anti-clockwise air circulation in zone A is observed. The center of the circulation moves towards wall W as the horizontal plane rises in the z direction (Figures 5a and 5b).

At the horizontal section $z/H = 0.29$, the air vortexes in zone B move clockwise regardless of the door position. In Figure 5a, it is noted that the direction of air circulation in zone B is strongly affected by the air rotation in zone A.

Figures 6a, 6b, and 6c present the contaminant concentration distributions for case 2B-1 for different horizontal

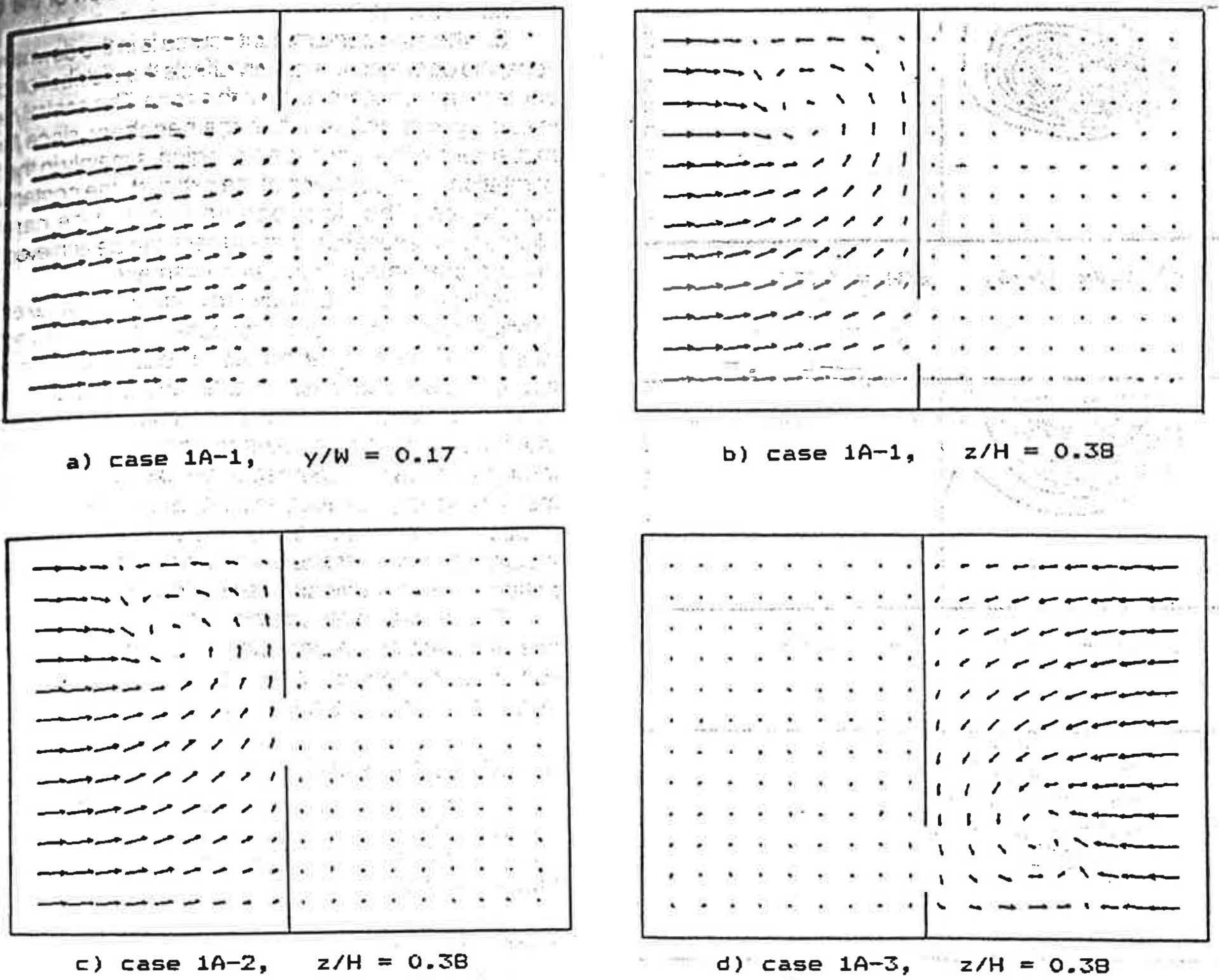
a) case 1A-1, y/W = 0.17

b) case 1A-1, z/H = 0.38

c) case 1A-2, z/H = 0.38

d) case 1A-3, z/H = 0.38

***Figure 3** Velocity vectors for the cases with the exhaust in zone A*

levels. At the lower level, $z/H = 0.13$, the contaminant has not yet been widely spread. As the horizontal level rises to $z/H = 0.29$ or higher, the contaminant covers the entire area of zone B. In case 2B-3 (Figure 6d), the contaminant concentration in the region near the partition is higher than that in case 2B-1 because the air has already been contaminated before reaching this area.

Exhaust and Contaminant Source in Zone A ($x_E/L = 0.19$, $y_E/W = 0.88$) Figures 7a, 7c, and 7e present the velocity vectors at the horizontal section of $z/H = 0.29$ for different door locations when the source and the exhaust opening are placed in zone A. It is observed that in zone A, air flows in a counterclockwise vortex, and the door location has a negligible effect on the flow pattern. This phenomenon can also be seen in Figures 7b and 7d. They show that the flow pattern in the vertical section at $y/W = 0.88$ for cases 2A-1 and 2A-3 is similar, though Figure 7d contains the door opening, while Figure 7b does not.

In zone B, which is no longer an active zone, the air velocities are significantly decreased. For case 2A-1, the door is not as close to the exhaust opening as for the other two cases, therefore the effect of the suction at the exhaust vent on the air movement at the door opening is less pronounced, which makes the air easier to enter zone B. As a result, the air movement in zone B is relatively strong in case 2A-1.

Figure 8a illustrates the contours of the contaminant concentration at $z/H = 0.29$ for case 2A-1. As described earlier, for case 2A-1, more contaminated air has a chance to enter zone B, therefore the contaminant concentration in zone B is significantly higher than in case 2A-3 (Figure 8b). Figures 8b and 8c show the contaminant distributions for case 2A-3 in two horizontal levels. At the lower level, zone B is almost free of contaminant. However, at the higher level, where the two zones are completely separated by the door soffit, there is some contaminant accumulation in the region near the ceiling of zone B. The reason for this is that the vortex in zone A, produced by the relative positions of the air supply and exhaust in zone A, restrains the migration of the contaminant to a certain extent, reducing the chance for the contaminant to enter zone B. The contaminant that has entered zone B is all moved upward by the air spiral and remains in the region near the ceiling.

CONCLUSION AND DISCUSSION

The effects of the door location on the airflow pattern and on the contaminant dispersion induced by natural and

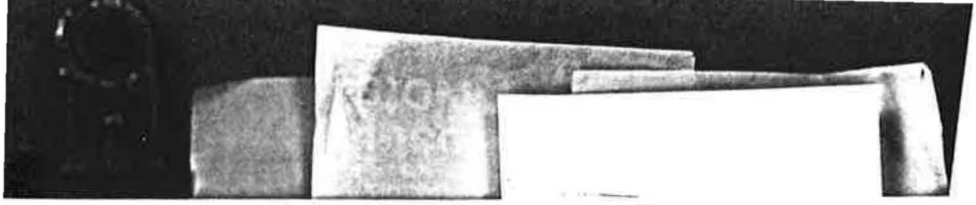

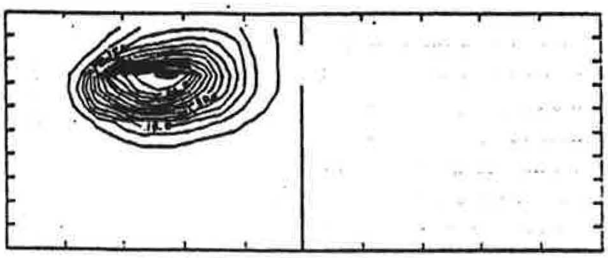

a) case 1A-3, z/H = 0.38

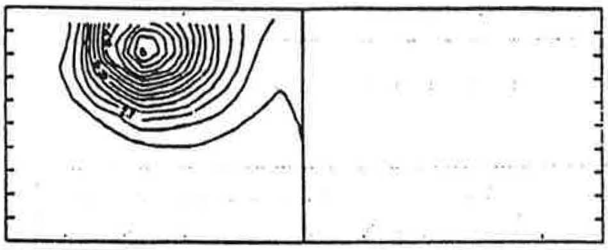

b) case 1A-3, z/H = 0.96

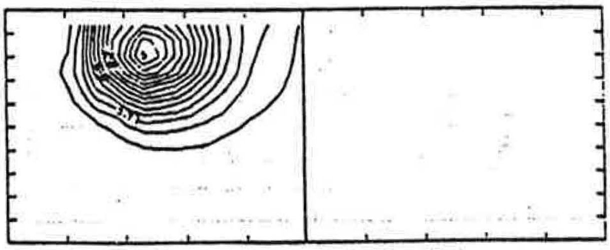

c) case 1A-1, z/H = 0.96

***Figure 4** Contours of the contaminant concentration for the cases with the exhaust in the zone A*

mechanical ventilation in a two-zone enclosure have been investigated. The door location not only guides the direction of the airflow but also affects the strength of the air circulation. Besides, since air serves not only as a diluter but also as a carrier of gaseous and particle contaminants such as smoke, dust, odors, and so on, the distribution of the contaminant concentration inevitably depends on the door location. The flow pattern and contaminant dispersion in a two-zone enclosure examined in the present paper can be summarized as follows:

1. The airflow pattern in the upstream zone, zone A (where either the air infiltration or the mechanical ventilation supply takes place) is not significantly influenced by the door location, while in the downstream zone, both the direction and the magnitude of the air circulation are dependent on the door location.

2. When the contaminant source is in the upstream zone, a partition combined with a local exhaust can efficiently protect the downstream zone from any contamination no matter where the door opening is. Even in the upstream zone, the contaminant could be confined in a small region if a proper arrangement of the supply and exhaust openings is made. Indeed, the air vortex in the upstream zone can restrain the dispersion of the contaminant around the source.

3. When the contaminant source is in the downstream zone, the door location greatly affects the distribution of the contaminant concentration in this zone. The central region is usually less polluted than the periphery, since the air movement in the downstream region is mainly in the form of rotation. The positions of the exhaust, the contaminant source, and the door opening should be carefully planned. A reasonable arrangement can be achieved from the comprehension of the air movement.

In this study, the buoyancy effect is not taken into consideration, and the temperature distribution is not provided. The buoyancy term must be added into the momentum equation whenever a contaminant source is also a heat source, such as a stove in a kitchen. For the cases of the first type of the air entering condition, the infiltration through the wall is assumed to be uniform. It may not be met in practice, however; as long as the velocity of the infiltration air can be considered to be one-dimensional, this assumption will not make a significant difference in the flow pattern and contaminant distribution.

The results obtained from this study have a practical relevance and give a clear picture and qualitative information about the ventilation air circulations and contaminant distributions in two-zone enclosures.

ACKNOWLEDGMENTS

We wish to express our thanks to the National Research Council of Canada and "Fonds Pour la Formation de Chercheurs et l'aide a la Recherche," which funded this study through the NSERC and the FCAR grants.

NOMENCLATURE

A = area
b = opening width
c = fraction of contaminant
c_μ = 0.09, a constant in turbulent model
e = contaminant emission rate (equal to unit)
g = gravity acceleration
H = room height
h = opening height
k = kinetic energy of turbulence
L = room length
l = $2h_iw_i/(h_i + W_i)$, length scale of turbulence at supply opening
l_E = the dimension of exhaust opening in x direction
n = normal direction
p = pressure
Re = Reynolds number, u_ih_i/ν
S_ϕ = source term for ϕ
t = time
u, v, w = velocity components in x, y, z directions
u_t = turbulent fluctuation velocity at supply opening
u_{IF} = infiltration velocity
u_i = air velocity at supply opening
x, y, z = cartesian coordinate system
W = width of room

Greek Symbols

ϵ = dissipation rate of k
μ_{eff} = effective dynamic viscosity
ν = kinematic viscosity
ρ = air density
ϕ = variable

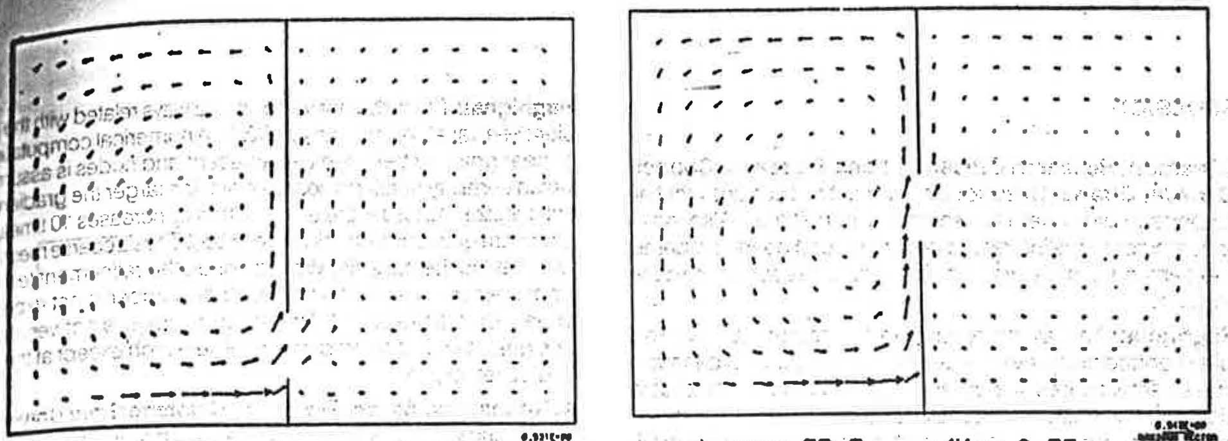

a) case 2B-1, z/H = 0.29

c) case 2B-2, z/H = 0.29

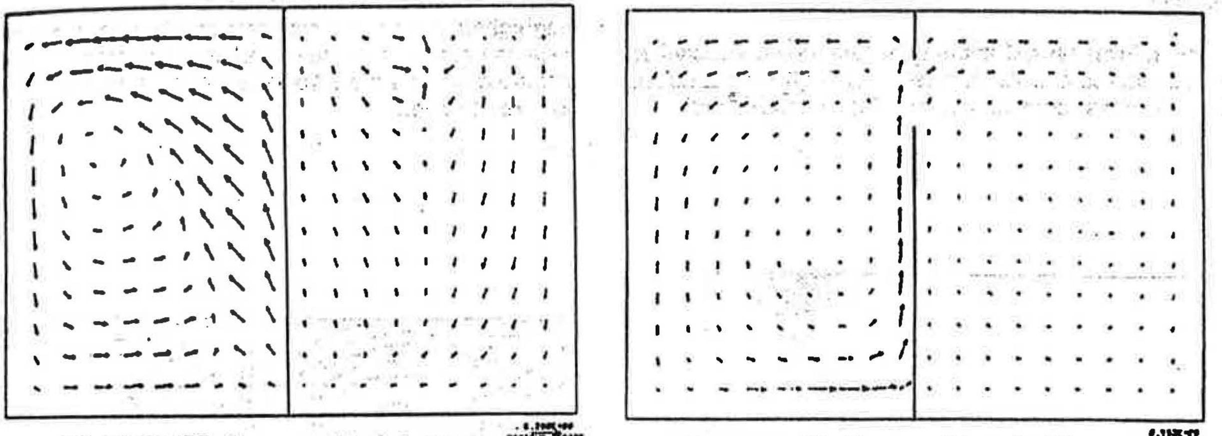

b) case 2B-1, z/H = 0.96

d) case 2B-3, z/H = 0.29

***Figure 5** Velocity vectors for the cases with the exhaust in the zone B*

Subscripts

D = door
E = exhaust opening
I = supply opening
s = source

REFERENCES

Berne, P., and Villand, M. 1987. "Prediction of air movement in a ventilated enclosure with 3-D thermahydraulic code TRIO." ROOMVET-87, Stockholm.

Chang, L.C.; Lloyd, J.R.; and Yang, K.T. 1982. "A finite difference study of natural convection in complex enclosures." *Proc. of 7th Int. Heat Transfer Conf.*, Vol. 2.

Chen, Q.Y.; Van der Kooi, J.; and Meyers, A. 1988. "Measurements and computations of ventilation efficiency and temperature efficiency in a ventilated room." *Energy and Building*, Vol. 12, pp. 85-99.

Davidson, L., and Olsson, E. 1987. "Calculation of age and local purging flow rate in rooms." *Building and Environment*, Vol. 22, pp. 111-127.

Gosman, A.D.; Nielsen, P.V.; Resting, A.; and Whitelaw, J.H. 1980. "The flow properties of rooms with small ventilation openings." *Transactions of the ASME*, Vol. 102, pp. 316-323.

Haghighat, F.; Jiang, Z.; and Wang, J.C.Y. 1989. "Natural convection and air flow pattern in a partitioned room with turbulent flow." *ASHRAE Transactions*, Vol. 95, Part 2.

Holmes, M.J. 1982. "The application of fluid mechanics simulation program PHOENICS to a few typical HVAC problems." Ove Arup and Partners, London, UK.

Horstman, R.H. 1988. "Predicting velocity and contamination distribution in ventilated volumes using Navier-Stokes equations." *Engineering Solutions to Indoor Air Problems*. Atlanta: American Society of Heating, Refrigerating, and Air-Conditioning Engineers, Inc.

Kato, S.; Murakami, S.; and Chirfu, S. 1986. "Study on air flow type clean room by means of numerical simulation and model test." IIS Annual Report of Group Research Activity on Numerical Simulation of Turbulent Flow, Number 2.

Kelkar, K.M., and Patankar, S.V. 1985. "Numerical prediction of natural convection in partitioned enclosures." *Numerical Heat Transfer*.

Launder, B.E., and Spalding, D. B. 1974. "The numerical computation of turbulent flows." *Comput. Meth. Appl. Mech. Eng.*, 3, pp. 269-289.

Lemaire, A.D. 1987. "The numerical simulation of the air movement and heat transfer in a heated room resp. a ventilated atrium." *Proc. of the Int. Conf. on Air Distribution in Ventilated Space, ROOMVENT-87*, Stockholm.

Markatos, N.C., and Pericleous, H.A. 1984. "Laminar and turbulent natural convection in a enclosed cavity." *Int. J. Heat and Mass Transfer*, Vol. 27, No. 5, pp. 755-772.

Nielson, P. V. 1981. "Contaminant distribution in industrial area with forced ventilation and two-dimensional flow." IIR-Joint Meeting, Commission EI, Essen, West Germany.

Rodi, W. 1984. *Turbulence models and their application in hydraulics—a state of the art review*, 2d rev. ed. Karlsruhe, Federal Republic of Germany.

DISCUSSION

J.T. Reardon, Research Officer, National Research Council of Canada, Ottawa, Ontario: Do I understand correctly that all the reported results were for isothermal conditions? Also, have your computer modeling results (reported here) been compared with experimental, measured data? The results reported are quite interesting.

F. Haghighat: Yes, all the results are for isothermal flow. The results reported here have not been compared with experimental measurement data since, so far, there are no experimental data available for a ventilated two-zone enclosure. However, the results for natural convection, obtained by the same numerical model, were compared with the reported text data, and they were in good agreement.

A.J. Baker, Professor, University of Tennessee, Knoxville: On your coarse computational mesh, would changing turbulent viscosity 10 times (larger or smaller) affect your solutions?

Haghighat: The turbulent viscosity is always related with the gradient of a variable, such as $\mu_t(\partial\theta/\partial x)$. In numerical computations a linear gradient between two adjacent grid nodes is assumed, which certainly results in some errors (the larger the gradient, or the cell size, the larger the error). When μ_t increases 10 times, the error from gradient term will be enlarged. Thus a coarse mesh system may not be suitable. We did not do the refinement test. For air movement in a room, the Reynolds number is not expected to be very high (about 10^4); therefore, the μ_t is not very large. Besides, the velocity gradient is not very high except at the inlet and outlet region.

A. Kirkpatrick, Assoc. Professor, Colorado State University, Fort Collins: For a situation with the contaminant in zone A, what is the reduction in overall contaminant concentration if the return duct is moved from zone A to zone B?

Haghighat: This is a very interesting question. We computed this case and noticed that the overall contaminant concentration increased in both zones. We can send you the detailed results if you are interested.

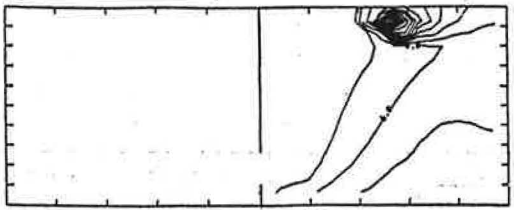

a) case 2B-1, z/H = 0.13

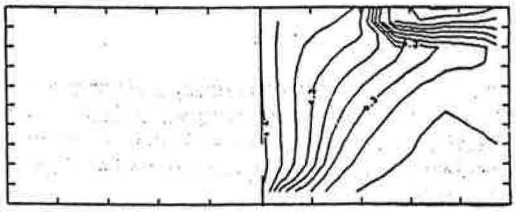

b) case 2B-1, z/H = 0.29

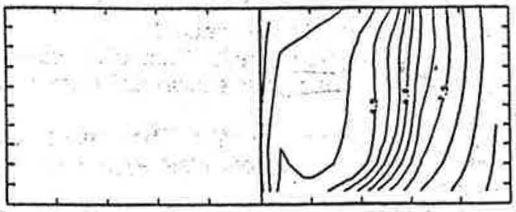

c) case 2B-1, z/H = 0.96

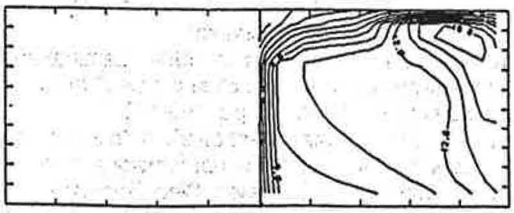

d) case 2B-3, z/H = 0.29

Figure 6 *Contours of the contaminant concentration for case 2B-1*

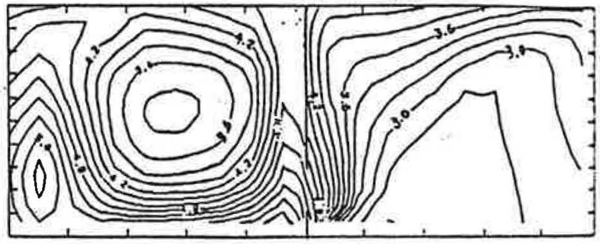

a) case 2A-1, z/H = 0.29

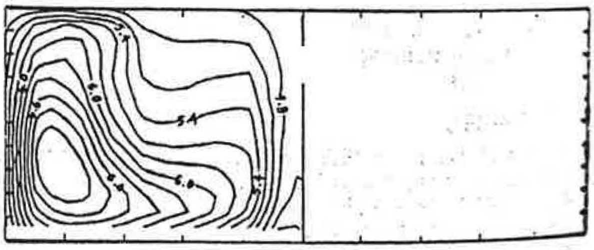

b) case 2A-3, z/H = 0.29

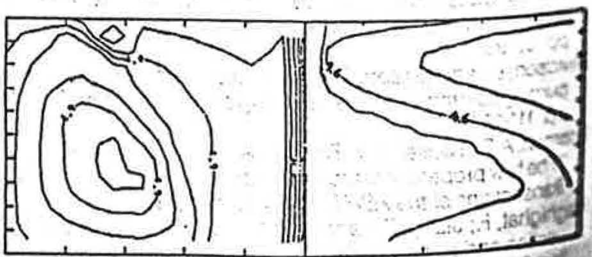

c) case 2A-3, z/H = 0.96

Figure 8 *Contours of the contaminant for the cases with the exhaust in the zone A*

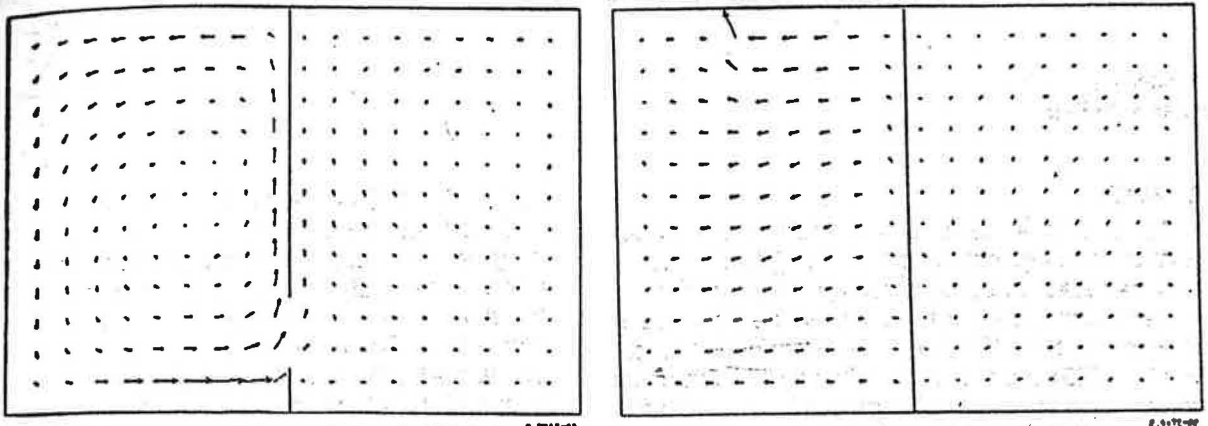

a) case 2A-1, z/H = 0.29

b) case 2A-1, y/W = 0.88

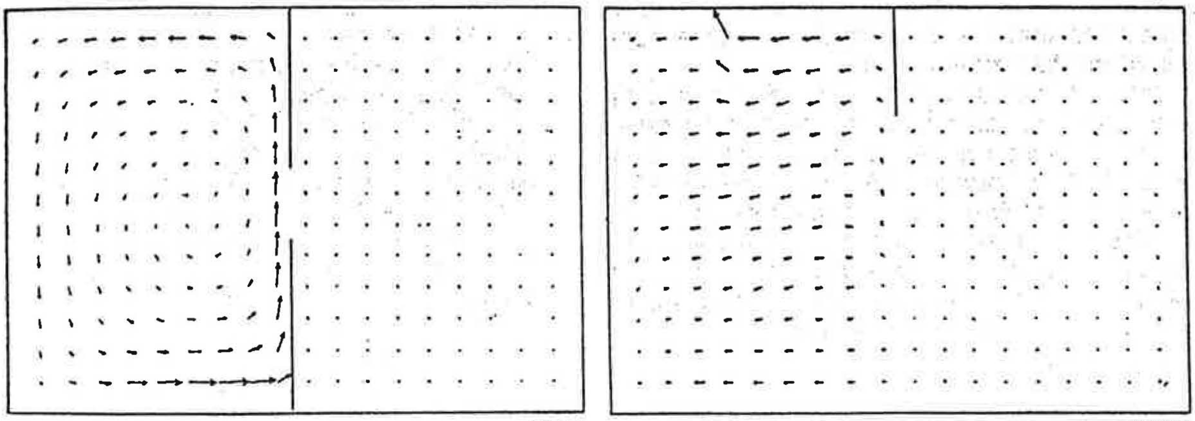

c) case 2A-2, z/H = 0.29

d) case 2A-3, y/W = 0.88

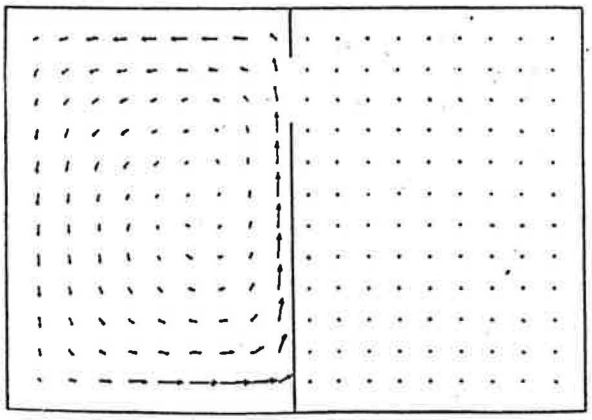

e) case 2A-3, z/H = 0.29

Figure 7 Velocity vectors for the cases with the exhaust in the zone A